Rotary Foil Propellers*

By

Neil Bose**

Abstract

A multiple stream tube theoretical model was developed for application to the rotary foil propeller. The outline of this method is described, together with the operation of a computer program which was written using this theoretical model. The basis of the method is for calculations on a two-dimensional rotary foil propeller. A three-dimensional development of the method was carried out by assuming elliptical loading across the span of the propeller blades.

The results are presented here for a series of propellers with a range of parameter variations and for two types of blade motion : a purely sinusoidal variation of the blade pitch angle relative to the undisturbed flow and a trochoidal motion as in the initial design of a rotary foil propeller model.

A design example is presented to show the approximate scale necessary for a full sized rotary foil propeller.

1. Introduction

A rotary foil propeller is similar in appearance to a horizontally mounted Voith-Schneider propeller, but unlike the Voith-Schneider propeller, it's blades describe a different oscillatory blade motion. The propeller is made up of a rotating disc mounted flush with the hull of a marine vehicle. Several straight blades extend from this disc and these blades are also able to rotate relative to the disc. The actual motion of the blades is an oscillatory one and can be controlled mechanically, electrically or hydraulically from behind the disc. In an actual application it is likely that either two of these propellers would be mounted back to back from a central skeg or that a single propeller might be mounted horizontally between two skegs. Figure 1 shows a diagramatical representation of such an arrangement. Figure 2 shows a side view of the type of oscillation of the blades as they rotate with the disc and as the propeller moves from right to left in the direction of F.

A U.K. patent application has been made for this design of propeller.

---

* Received April, 30, 1987

** Lecturer, Department of Naval Architecture & Ocean Engineering, University of Glasgow

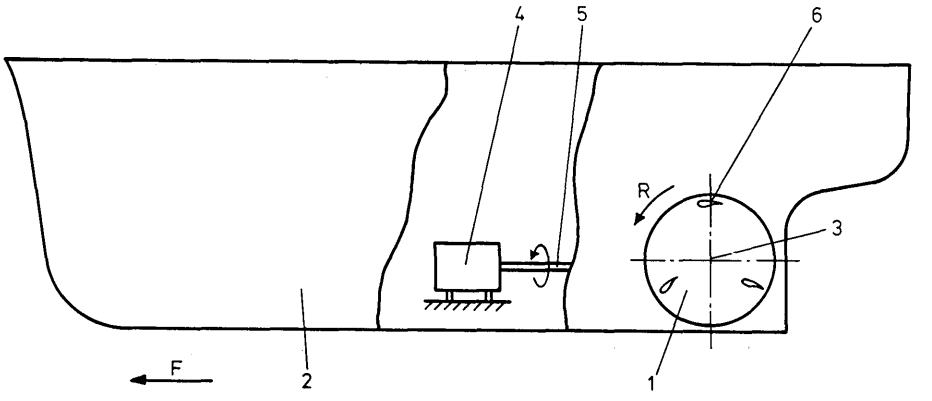

Fig. 1 Diagramatic Representation of a Rotary Foil Propeller

1-Rotary Foil Propeller
2-Ship Hull
3-Propeller Axis
4-Engine
5-Propeller Shaft
6-Propeller Blade
7-Position of Zero Blade Pitch
F-Direction of Forward Motion
R-Direction of Rotation

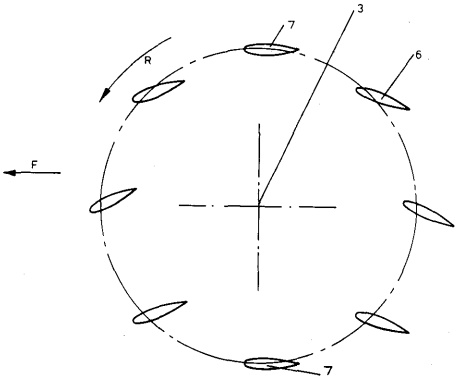

Fig. 2 Side View Depicting the Form of the Blade Oscillation

2. Multiple Stream Tube Theory for a Rotary Foil Propeller

A multiple stream tube approach was adopted and developed for the rotary foil propeller from the theory developed for vertical axis wind turbines originally by Strickland[1] and Shankar[2] with later additions by Read and Sharpe[3]. A review of this theory, its refinements and applications to vertical axis wind turbines was given by Sharpe[4] in 1984.

The theory assumes that there are two 'actuator discs' in tandem at the upstream and downstream blade passes. The flow through the propeller is assumed to be straight, enabling each streamline to be designated by the angle, it makes with the radius of the propeller, θ, (Fig.3). It is assumed that the free stream pressure p_a is attained at some point inside the propeller on each streamline, and the velocity at that point V_a is taken as the velocity in the wake for the upstream actuator and the free stream velocity for the downstream actuator. Each stream tube is enclosed by two streamlines at θ and $\theta+\delta\theta$ (Fig.4).

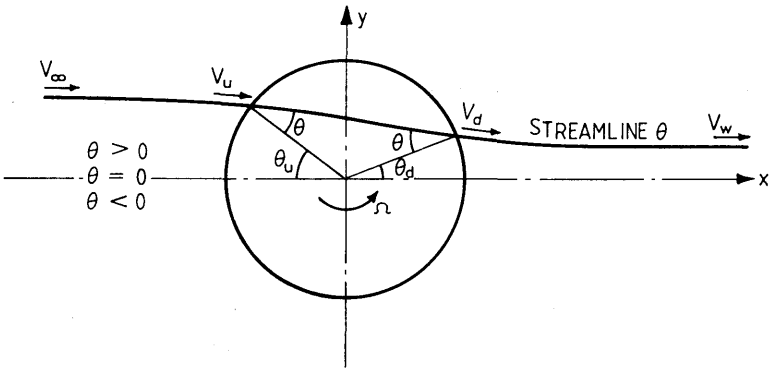

Fig. 3 Flow through the Propeller

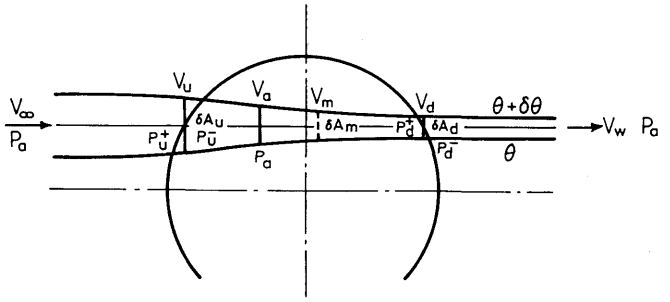

Fig. 4 Flow through an Elemental Streamtube

A two dimensional slice of unit length perpendicular to the x-y plane is considered. The parameters, number of blades (N), radius (R) (this is the pitch radius of the propeller blades) and chord length (c) define the turbine solidity $\sigma=\frac{Nc}{R}$. The theory is valid strictly, only for a large number of blades, the effect of the blades is 'smeared' around the circumference of the circle of the propeller. The propeller is assumed to be operating in a stream of uniform velocity V_∞ and at a blade 'tip' speed ratio $TSR=\frac{R\Omega}{V}$ where Ω is the angular velocity of the propeller. The flow is assumed to be steady at each instant of time and as such the effects of changes in the circulation around the blades is neglected.

2.1 Calculation of the Upstream and Downstream Velocities in the Stream Tube

Application of Bernoulli's Equation to the three parts of the stream tube gives (at the same potential height)

$$\frac{1}{2}\rho V_u^2+P_u^+=\frac{1}{2}\rho V_\infty^2+P_a \tag{1}$$

$$\frac{1}{2}\rho V_u^2+P_u^-=\frac{1}{2}\rho V_a^2+P_a=\frac{1}{2}\rho V_d^2+P_d^+ \tag{2}$$

$$=\frac{1}{2}\rho V_w^2+P_a=\frac{1}{2}\rho V_d^2+P_d^- \tag{3}$$

From these, the thrust forces at the upstream and downstream actuators can be found as

$$\delta T_u=(P_u^- -P_u^+)\,\delta A_u=\frac{1}{2}\rho\,(V_a^2-V_\infty^2)\,\delta A_u \tag{4}$$

$$\delta T_d=(P_d^- -P_d^+)\,\delta A_d=\frac{1}{2}\rho\,(V_w^2-V_a^2)\,\delta A_d \tag{5}$$

If the streamtube is assumed to be straight along its length, these thrust forces can also be found from the rate of change of momentum.

$$\delta T_u=(\rho V_u\delta A_u)\,(V_a-V_\infty) \tag{6}$$

$$\delta T_d=(\rho V_d\delta A_d)\,(V_w-V_a) \tag{7}$$

Equating equations (4) and (6), and (5) and (7) gives

$$V_u=\frac{1}{2}(V_a+V_\infty) \tag{8}$$

$$V_d=\frac{1}{2}(V_w+V_a) \tag{9}$$

and hence

$$V_d-V_u=\frac{1}{2}(V_w-V_\infty) \tag{10}$$

Assuming that V_u and V_d are parallel to the x-axis ($\theta\approx\theta_u\approx\theta_d$) which is approximately true for light to moderately loaded propellers (these type of propellers are by their design lightly loaded) the thrust on the upstream and downstream blades can be resolved from the blade element lift and drag forces as (Fig. 5)

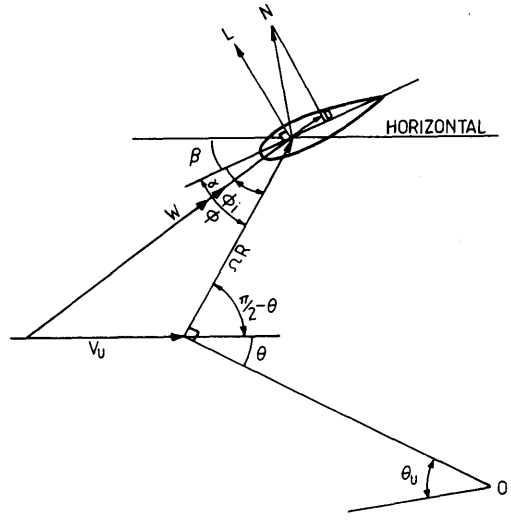

Fig. 5 Relative Velocity Triangle

$$\delta T_{bu} = \delta L_u \cos(\theta + \phi_{iu}) - \delta D_u \sin(\theta + \phi_{iu}) \quad (11)$$

$$\delta T_{bd} = \delta L_d \cos(\theta + \phi_{id}) - \delta D_d \sin(\theta + \phi_{id}) \quad (12)$$

Where θ is +ve above the x-axis and -ve below the x-axis.

The lift and drag for a two dimensional slice of blade of unit length can be written as

$$L = \frac{1}{2}\rho c W^2 C_L \quad (13)$$

$$D = \frac{1}{2}\rho c W^2 C_D \quad (14)$$

where W is the inflow velocity to the blade. Multiplying (13) and (14) by N, the number of blades, gives the total lift and drag forces generated by the propeller blades at each position (θ), but it is necessary to calculate the effect of these blade element forces over the stream tube area. This is done by multiplying the blade element values by the fraction of the projected streamtube area (per unit length of the propeller) to the circumference of the propeller,

$$\frac{\delta A_u \sec\theta}{2\pi R} \text{ and } \frac{\delta A_d \sec\theta}{2\pi R}$$

Hence on the upstream stream tube element

$$\delta T_u = \frac{1}{2}\rho N c W_u^2 \frac{\delta A_u \sec\theta}{2\pi R}\left[C_L \cos(\theta + \phi_{iu}) - C_D \sin(\theta + \phi_{iu})\right] \quad (15)$$

From equations (6) and (8)

$$\delta T_u = \rho V_u \delta A_u (V_a - V_\infty) = 2\rho V_u \delta A_u (V_u - V_\infty) \quad (16)$$

Equating (15) and (16) and writing the solidity

$$\sigma = \frac{Nc}{R}$$

gives

$$2V_u(V_u - V_\infty) = \frac{\sigma}{4\pi} W_u^2 \sec\theta\left[C_L \cos(\theta + \phi_{iu}) - C_D \sin(\theta + \phi_{iu})\right] \quad (17)$$

and similarly for the downstream stream tube element

$$2V_d(V_d - V_a) = \frac{\sigma}{4\pi} W_d^2 \sec\theta\left[C_L \cos(\theta + \phi_{id}) - C_D \sin(\theta + \phi_{id})\right] \quad (18)$$

For a given tip speed ratio, free stream velocity and propeller solidity and if the foil section lift and drag coefficients are known for a range of angles of attack (assuming quasi-steady conditions), equation (17) can be solved by iteration to obtain V_u. V_a can then be found from equation (8) and V_d, again by iteration from equation (18).

In order to do this it is necessary to calculate the following quantities

$$\phi_{iu} = tan^{-1}\left(\frac{V_u + \Omega R sin\theta}{\Omega R cos\theta}\right) - \theta$$

$$W_u^2 = \left(V_u + \Omega R sin\theta\right)^2 + \left(\Omega R cos\theta\right)^2$$

$$\phi_{id} = tan^{-1}\left(\frac{V_d + \Omega R sin\theta}{\Omega R cos\theta}\right) - \theta$$

$$W_d^2 = \left(V_d + \Omega R sin\theta\right)^2 + \left(\Omega R cos\theta\right)^2$$

where θ is +ve above the x-axis and −ve below the x-axis.
Also, $\phi_i = \pi/2 - \theta - \beta - \alpha$ (upstream and downstream) where β is the blade angle to the horizontal and α is the angle of attack (Fig. 5).

2.2 **Blade angle**

Two types of blade motion were considered. The blade pitch angle β is measured between the blade chord line and the horizontal.

i) Sinusoidal blade motion

In this the blade pitch changed in a manner such that

$$\beta = \beta_{max}\ cos\ \theta$$

where β_{max} was the maximum blade pitch angle and θ was the angle of the blade position from the x-axis. The blade angle β was equal to zero at the extreme upper and lower positions of the blade (shown as 7 on Figure 2). The maximum blade angle occurred at a blade position $\theta = 0$ as the blades cross the x-axis.

ii) Trochoidal blade motion

The actual rotary foil propeller model was constructed with a mechanism which controls the pitch angle of the blades such that this angle follows the slope of a trochoidal curve. Again a blade pitch of zero occurs at the extreme upper and lower positions, but the maximum blade pitch, β_{max}, occurs at an angle of $\theta = -\beta_{max}$, a blade position β_{max} below the x-axis. The blade angle is given by :

$$\beta = tan^{-1}\left(\frac{sin\beta_{max}\ cos\theta}{1 + sin\beta_{max}\ sin\theta}\right)$$

2.3 Power Absorbed by the Propeller

The power absorbed on each streamtube on both the upstream and downstream sides of the propeller is given by

$$Power = \frac{\Omega R}{4\pi}\rho\sigma\ sec\theta\left(W_u^2\ \delta A_u\ (C_{Lu}\ sin\phi_{iu} + C_{Du}\ cos\phi_{iu})\right.$$
$$\left. + W_d^2\ \delta A_d\ (C_{Ld}\ sin\phi_i + C_{Dd}\ cos\phi_{id})\right) \qquad (19)$$

V_m is defined to be the fluid velocity where the cross section of the stream tube bounded by stream lines θ and $\theta+\delta\theta$ is

$$\delta A_m = R\ cos\theta d\theta \tag{20}$$

Also it is assumed that

$$\delta A_u + \delta A_d = 2\delta A_m \qquad \text{for each stream tube}$$

In incompressible flow, $V\delta A$=constant, for each stream tube and hence

$$\delta A_u\ V_u = \delta A_d\ V_d = \delta A_m\ V_m = const.$$

$$2\delta A_m = \delta A_u + \delta A_d = \frac{\delta A_m\ V_m}{V_u} + \frac{\delta A_m\ V_m}{V_d}$$

$$V_m = \frac{2\ V_u\ V_d}{V_u + V_d}$$

From (20) $\delta A_m = R\ cos\theta\ \delta\theta = \dfrac{\delta A_u\ V_u}{V_m}$

$$\delta A_u\ sec\theta = \frac{R\delta\theta\ V_m}{V_u} = \frac{2\ V_d\ R\ \delta\theta}{(V_u + V_d)} \tag{21}$$

Similarly $\delta A_d\ sec\theta = \dfrac{R\delta\theta\ V_m}{V_d} = \dfrac{2\ V_u\ R\ \delta\theta}{(V_u + V_d)}$ (22)

Substitution of (21) and (22) into the equation for power (19) gives

$$Power = \frac{\sigma}{2\pi}\rho\frac{\Omega\ R^2\ \delta\theta}{(V_u + V_d)}\Big(W_u^2\ V_d\ (C_{Lu} sin\ \phi_{iu} + C_{Du} cos\ \phi_{iu}) + W_d^2\ V_u\ (C_{Ld}\ sin\ \phi_{id} + C_{Dd}\ cos\ \phi_{id})\Big)$$

This equation can be integrated over the blade position angle θ in the range $-\pi/2 \leqq \theta \leqq \pi/2$ to obtain the total power absorbed by a two-dimensional segment of the propeller.

2.4 Thrust Developed by the Propeller

Combination of equation (15) and its counterpart for the downstream streamtube element with equations (21) and (22) leads to equations for thrust on the propeller.

On the upstream streamtube element,

$$\delta T_u = \frac{\rho\sigma\ W_u^2\ V_d\ R\ \delta\theta}{2\pi\ \ (V_u + V_d)}\Big(C_{Lu}\ cos\ (\theta + \phi_{iu}) - C_{Dd}\ sin\ (\theta + \phi_{iu})\Big) \tag{23}$$

and on the downstream streamtube element

$$\delta T_d = \frac{\rho\sigma\ W_d^2\ V_u\ R\ \delta\theta}{2\pi\ \ (V_u + V_d)}\Big(C_{Ld}\ cos\ (\theta + \phi_{id}) - C_{Dd}\ sin\ (\theta + \phi_{id})\Big) \tag{24}$$

These two equations can be integrated over $-\pi/2 \leqq \theta \leqq \pi/2$ to obtain the total thrust on the upstream and downstream sides of the propeller.

2.5 Propeller Coefficients

Thrust and torque were non-dimensionalised into the following thrust and torque coefficients.

$$T_c=\frac{T}{Area\ \rho\ \Omega^2R^2} \tag{25}$$

$$Q_c=\frac{Q}{Area\ \rho\ \Omega^2R^3} \tag{26}$$

Where Area —swept frontal area of the propeller (=2R for the 2-D propeller)

T —total thrust

Q —total torque $\left(=\frac{\text{total power}}{\Omega}\right)$

Propeller efficiency

$$\eta=\frac{Useful\ Work}{Absorbed\ Power}=\frac{TV}{\Omega Q}=\frac{T_cJ}{Q_c\pi}$$

where J is the advance ratio

$$J=\frac{\pi V}{\Omega R}=\frac{\pi}{TSR}$$

2.6 Vertical Force on the Propeller

Resolution of the forces on the propeller blades into the vertical direction led to two equations for the calculation of the vertical force on the upstream and downstream sides of the propeller (upwards taken as +ve).

On the upstream tube element

$$\delta VF_u=\frac{\rho\sigma\ W_u^2\ V_d\ R\ \delta\theta}{2\pi\ \ (V_u+V_d)}\left(C_{Lu}\ sin\ (\theta+\phi_{iu})+C_{Du}\ cos\ (\theta+\phi_{iu})\right) \tag{27}$$

and on the downstream streamtube element

$$\delta VF_d=-\frac{\rho\sigma\ W_d^2\ V_u\ R\ \sigma\theta}{2\pi\ \ (V_u+V_d)}\left(C_{Ld}\ sin\ (\theta+\phi_{id})+C_{Dd}\ cos\ (\theta+\phi_{id})\right) \tag{28}$$

2.7 Normal and In-line Forces on Propeller Blades

Again resolution of the lift and drag forces on each blade leads to equations for the normal and in-line forces on each propeller blade.

Normal force on upstream blade, (upwards +ve)

$$\delta N_u=\frac{\rho\sigma\ W_u^2\ V_d\ R\ \delta\theta}{2\pi N\ \ (V_u+V_d)}\left(C_{Lu}\ cos\ \alpha_u+C_{Du}\ sin\ \alpha_u\right) \tag{29}$$

normal force on downstream blade,

$$\delta N_d = -\frac{\rho\sigma\ W_d^2\ V_u\ R\ \delta\theta}{2\pi N\ \ (V_u+V_d)}\left(\ C_{Ld}\ cos\ \alpha_d + C_{Dd}\ sin\ \alpha_d\ \right) \tag{30}$$

in-line force on upstream blade (towards trailing edge +ve),

$$\delta LF_u = \frac{\rho\sigma\ W_u^2\ V_d\ R\ \delta\theta}{2\pi N\ \ (V_u+V_d)}\left(\ -C_{Lu}\ sin\ \alpha_u + C_{Du}\ cos\ \alpha_u\ \right) \tag{31}$$

in-line force on downstream blade

$$\delta LF_d = \frac{\rho\sigma\ W_d^2\ V_u\ R\ \delta\theta}{2\pi N\ \ (V_u+V_d)}\left(\ -C_{Ld}\ sin\ \alpha_d + C_{Dd}\ cos\ \alpha_d\ \right) \tag{32}$$

3. Foil Section Data

The foil section data used in the calculations were based on experimental data for the NACA 0012 section. Since the main calculations were made for a model scale propeller, the data used were that for a Reynolds number of 8×10^4. However, data for this section above an angle of attack of 25^0 were not available at this Reynolds number, so the data for a Reynolds number of 3×10^5 were used in the range of angles of attack from 25^0 to 180^0 . The data were obtained from the papers of Sharpe[5] and Shankar[2] after the work of Critzos et al[3] and Jacobs and Sherman[7]. The lift and drag coefficients are presented in Table 1 and the lift coefficient to an angle of attack of 40^0 is shown in Figure 6, together with data for higher Reynolds number.

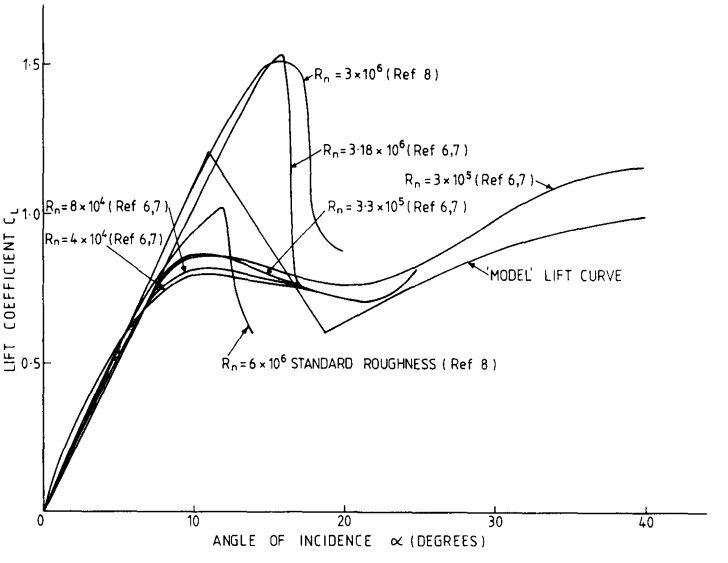

Fig. 6 Lift Curves for Section NACA 0012

Table 1 Lift and Drag Data for the NACA 0012 Section

α	C_L	C_D
0.0	0.00	0.0180
1.0	0.10	0.0180
2.0	0.20	0.0175
3.0	0.31	0.0175
4.0	0.42	0.0175
5.0	0.52	0.0180
6.0	0.61	0.0195
7.0	0.70	0.0220
8.0	0.755	0.0285
9.0	0.790	0.0355
10.0	0.815	0.0555
11.0	0.820	0.090
12.0	0.810	0.130
13.0	0.805	0.150
14.0	0.790	0.170
15.0	0.780	0.190
16.0	0.770	0.210
17.0	0.755	0.230
18.0	0.745	0.250
19.0	0.725	0.268
20.0	0.720	0.290
21.0	0.710	0.310
22.0	0.700	0.335
23.0	0.720	0.360
24.0	0.765	0.385
25.0	0.810	0.41
30.0	0.975	0.59
40.0	1.15	0.96
50.0	1.08	1.30
60.0	0.94	1.58
70.0	0.68	1.80
80.0	0.40	1.92
90.0	0.06	1.93
100.0	−0.25	1.88
110.0	−0.55	1.76
120.0	−0.80	1.55
130.0	−0.98	1.30
140.0	−1.05	0.96
150.0	−0.95	0.60
160.0	−0.66	0.28
170.0	−0.92	0.10
180.0	0.00	0.01

For full sized propellers operating at higher Reynolds number, the maximum lift coefficient would be larger. Since the angle of attack of the propeller blades varies from beyond stall to negative values during operation, any increase in size of this range or increase in the maximum lift coefficient will increase the performance of the propeller. Calculations based on foil section data for a Reynolds number of 8×10^4 will give conservative results if the propeller coefficients are scaled up to full size.

Dynamic stall will also affect the performance of the propeller. No allowance was made for dynamic stall in the calculations. For a foil section operating with an oscillating angle of attack from the unstalled region just into stall and back to the unstalled region, the level of maximum lift coefficient would be expected to be higher than for the same section at a steady angle of attack over a similar range. These effects would also be expected to improve the performance of the propeller over that calculated.

4. Calculations on Two Dimensional Propellers

Figures 7 and 8 show the results from calculations on a propeller with the following characteristics.

$$\textit{Consisting of}\begin{cases}\textit{Solidity}=0.9\\ \textit{No. of Blades}=3\\ \textit{Chord Length}=0.03m\\ \textit{Radius}=0.1m\end{cases}$$
$$\textit{Free stream velocity}=2.0m/s$$

Calculations were carried out for fresh water (density=1000 kg/m^3). A Reynolds number was calculated using a kinematic viscosity of water of 0.1146×10^{-5}, but the Reynolds number is only used to judge which foil section data should be used and does not directly affect the calculation.

Blade Pitch Angle		Blade Pitch Variation	
Degrees	Radians	Trochoidal	Sinusoidal
0	0.0	✓	
5	0.087	✓	✓
10	0.175	✓	✓
15	0.262	✓	✓
20	0.349	✓	✓
30	0.524	✓	✓
40	0.698	✓	
50	0.873	✓	
60	1.047	✓	

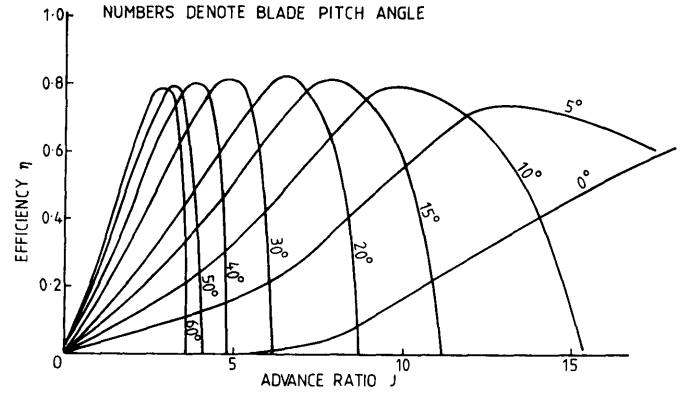

a. Efficiency η

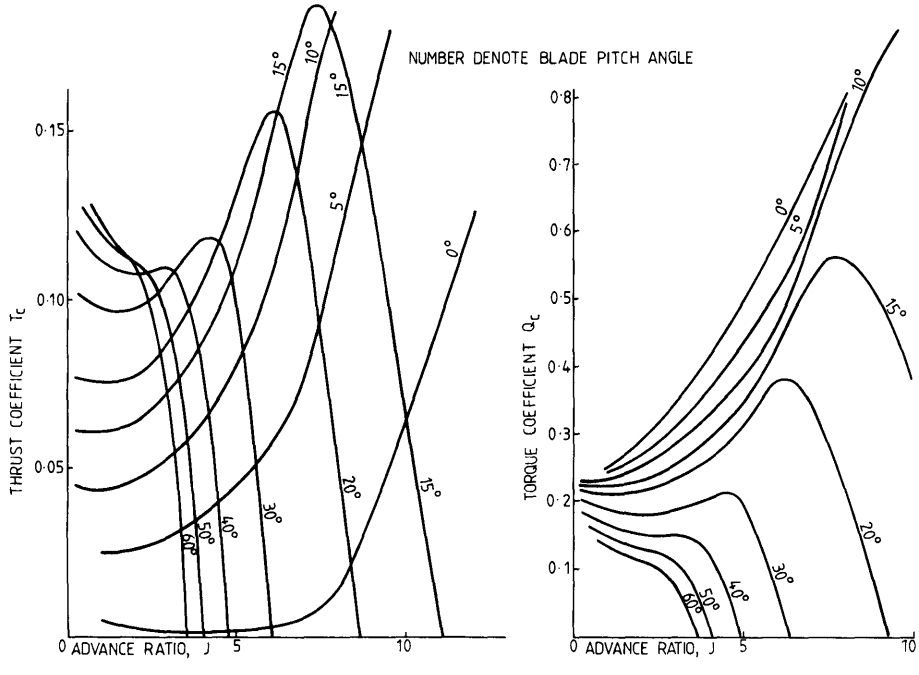

b. Thrust Coefficient Tc　　c. Torque Coefficient Qc

Fig. 7 Rotary Foil Propeller Model—Trochoidal Pitch Variation

The calculations were carried out for the maximum blade pitch angles shown below for both sinusoidal and trochoidal blade pitch variation.

Figures 7a, b and c show the efficiency, thrust coefficient and torque coefficient plotted against advance ratio for a propeller with a trochoidal variation of blade pitch angle. Figures 8a, b and c show similar curves of the comparison between a propeller with a trochoidal variation of pitch angle and a sinusoidal variation of pitch angle.

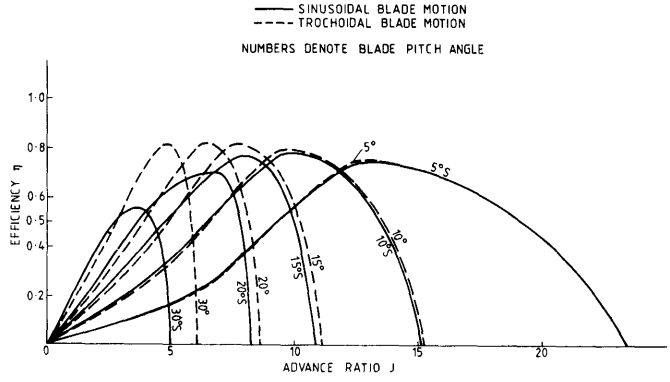

a. Efficiency η

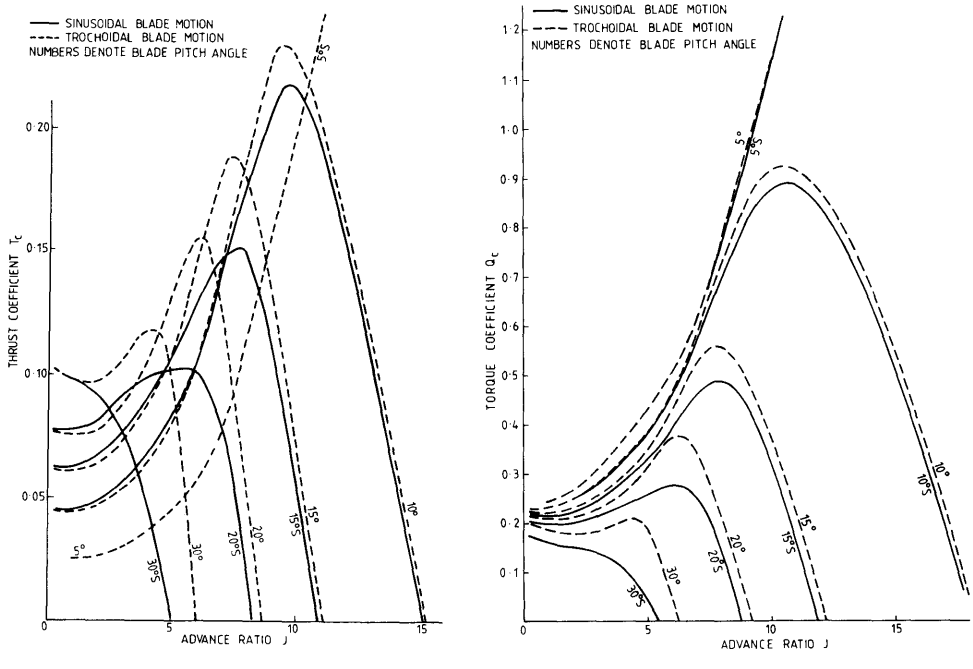

b. Thrust Coefficient Tc

c. Torque Coefficient Qc

Fig. 8 Rotary Foil Propeller Model—Comparison of Blade Motions (Solidity=0.9)

With the trochoidally varied blades, the maximum efficiency reached is just over 0.8. Maximum efficiencies of around 0.8 are attained over a wide variation of maximum blade pitch angle from 10-60 degrees. The maximum efficiency of 0.82 is reached with a propeller with a maximum blade pitch angle of 20 degrees. The peak in the efficiency curves lies at lower values of advance ratios the higher the maximum blade pitch angle. Propulsive forces are achieved with propellers whose maximum blade pitch angle is very low or zero,

but only at very high advance ratios.

The situation is different for the propeller with sinusoidally varying blade pitch angle. The maximum efficiency is always lower than for the trochoidally varied blades except as the maximum blade pitch angle is reduced below 5 degrees when the efficiencies become equal (the propeller blade motion is the same for $\beta_{max}=0$). The maximum efficiency reduces as the maximum blade pitch angle is increased (at $\beta_{max}=30^0$, the peak in the efficiency curve has reduced to 0.55, Figure 8a). Also the range of advance ratios over which positive thrust is produced is less than with the trochoidally varied blades. For a propeller with a maximum blade pitch angle of 20 degrees, the maximum efficiency is 0.7 as compared to 0.82 for the trochoidally varied blades. Figures 8b and c show the comparison between thrust and torque coefficients for the two types of propeller.

For calculations carried out with the same foil section data, changes in free stream velocity, radius, chord length and number of blades, do not affect the calculated values of efficiency, thrust coefficient and torque coefficient if the solidity remains unchanged. Changes in radius and free stream velocity at constant solidity do, however, affect the absolute values of thrust and torque of the propeller. The only meaningful change is a change in propeller solidity. Figures 9a, b and c show the results of efficiency, thrust coefficient and torque coefficient plotted against advance ratio for a propeller with varying solidity (from 0.3 to 1.8) and for a maximum blade pitch angle of 20 degrees. Figure 9a shows that variation in solidity causes only a small variation in efficiency at the peak of the efficiency curve ; a variation of about 3% in the peak efficiency over this solidity range. Figures 9b and c, however, show that the thrust and torque coefficients vary more or less linearly with solidity at any given value of advance ratio.

The teory, however, is valid only for streamlined flow and for small slip-stream contractions. It allows for the effect of blades by 'smearing' their effect around the circumference of the propeller. Large solidities will inevitably mean large blade chords in a practical propeller design. The predicted performance at very high solidities should therefore be treated with some caution. The theory does not allow for the periodicity of the flow encountered with a real propeller with a finite number of blades.

Figures 10 and 11 show the variation of power, thrust and vertical force acting on the whole propeller. Figures 12 shows the variation of normal and in-line force acting on a single blade of the propeller. These calculations were carried out by varying the number of blades and the chord length at a constant value of solidity. The solidity was 0.9, the maximum blade oscillation angle was 20 degrees and the advance ratio was 6.5. The power, thrust, angular

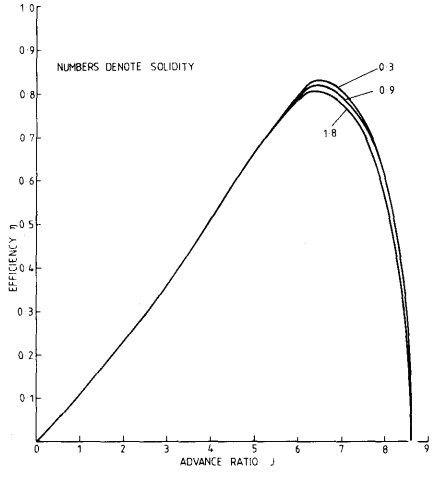

a. Efficiency against Advance Ratio

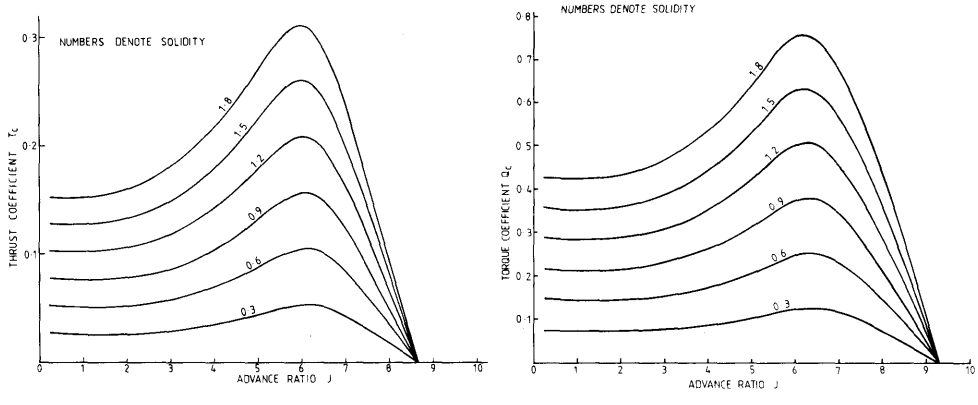

b. Thrust Coefficient against Advance Ratio c. Torque Coefficient against Advance Ratio

Fig. 9 Rotary Foil Propeller Model—Variation of Solidity at Bmax-0.349

velocity, efficiency (=0.82), thrust coefficient and torque coefficient was the same for all these propellers. The radius was 0.1m and the free stream velocity 2.0m/s. Table 2 shows the values of the number of blades and chord lengths. Again the blade angle variation was trochoidal.

Figure 10 shows the comparison between propellers with 2, 3 and 4 blades ; Figure 11 shows the comparison between propellers with 3, 4, 5 and 10 blades. The calculations were carried out in such a way that the values for propellers with 2, 3, 4, 6, 8, 12, etc. blades were obtained 'exactly' while propellers with 5 and 10 blades had to rely on data interpolated between stream tube positions at 7.5 degree intervals.

Figure 10 shows the huge variations in power, thrust and vertical force with

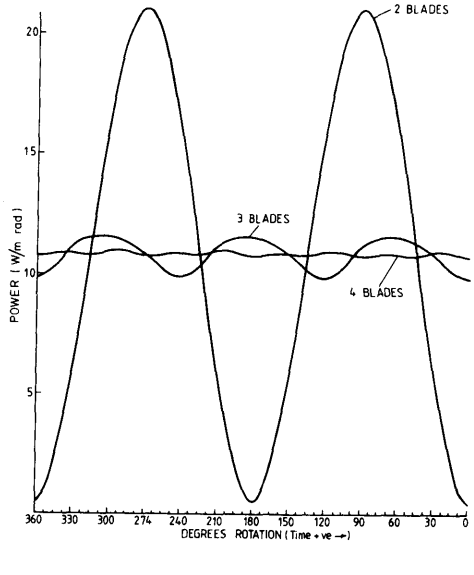

Fig. 10a Comparison of Power on Propeller at Const. Solidity

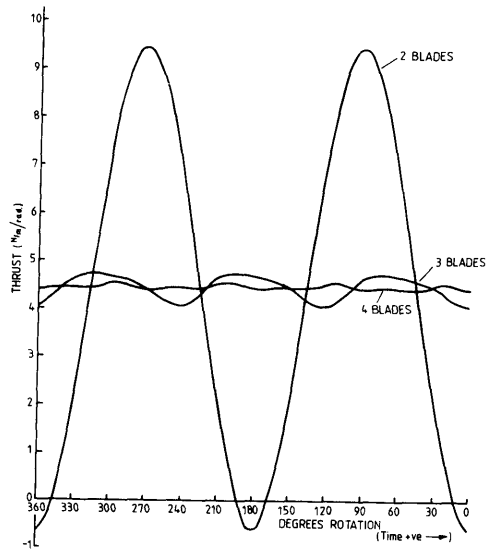

10b Comparison of Thrust Force on Propeller at Const. Solidity

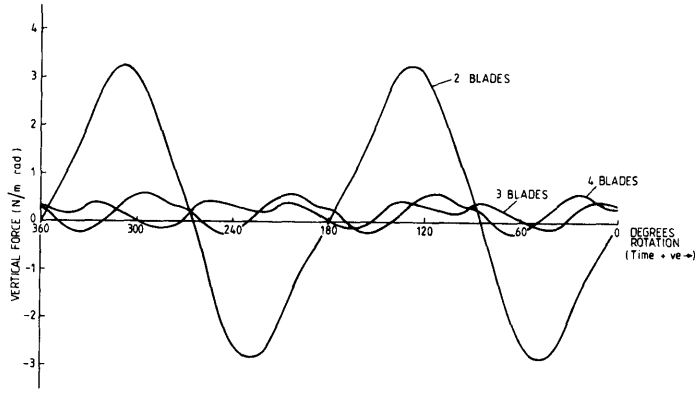

10c Comparison of Vertical Force on Propeller at Const. Solidity

propeller rotation that are a feature of two bladed propeller. Three and more bladed propellers have a much smoother variation of these parameters with their rotation. Figure 11 is a similar plot of a part of the cycle which shows that while power and thrust variations are much reduced below those of a three bladed propeller, the vertical force variation is actually greater with a 4-bladed propeller than with a 3-bladed propeller. As would be expected a 10 bladed propeller has very smooth power, thrust and vertical force characteristics. With all of these propellers a small mean positive vertical force was estimated.

For propellers with 3, 4 and 5 blades, Figure 12 shows the variation of the

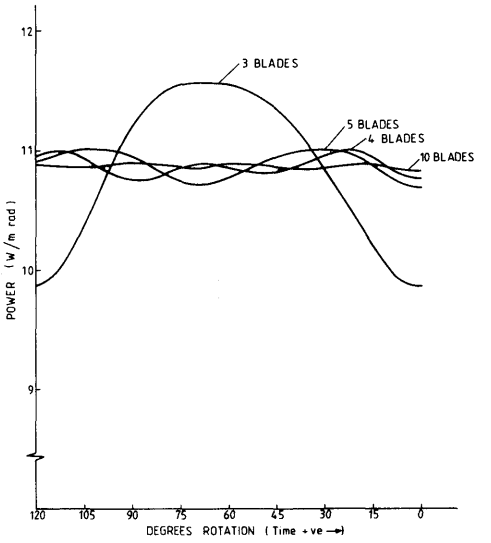

Fig. 11a Comparison of Power on Propeller at Const. Solidity

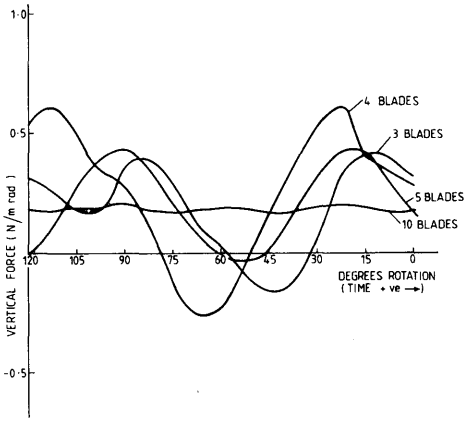

11b Comparison of Thrust Force on Propeller at Const. Solidity

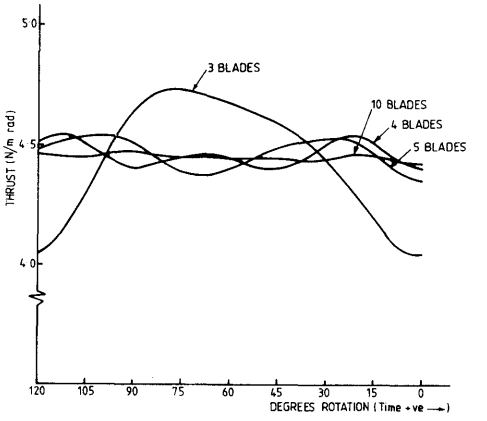

11c Comparison of Vertical Force on Propeller at Const. Solidity

normal and in line force acting on one blade of the propeller. The amplitude of these variations is approximately inversely proportional to the number of blades. The forces are slightly greater on the upstream side of the propeller. The normal force varies approximately sinusoidally with time. The in line blade force varies approximately as $sin\left(\frac{3\theta}{2}\right)$ where θ is the blade position angle.

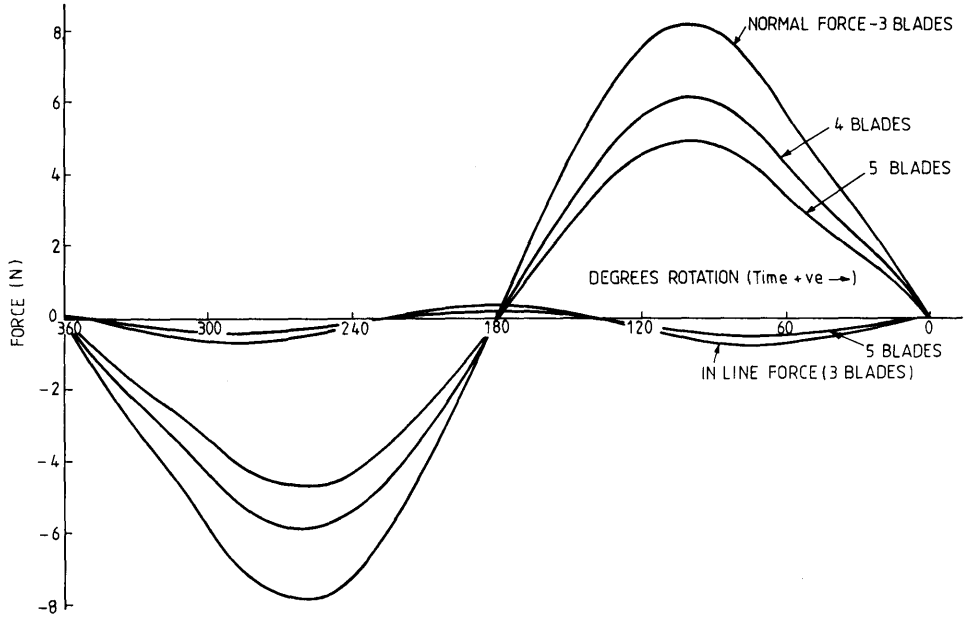

Fig. 12 Normal and In-line Force on Propeller Blade during One Cycle

Table 2 Variation of Chord Length with Solidity for Propellers with Varying Number of Blades

No. of Blades	2	3	4	5	10
Chord Length (m)	0.0450	0.0300	0.0225	0.0180	0.0090

5. Calculations on a Three Dimensional Propeller

An estimation of the effects of finite blade span was obtained by assuming that the distribution of circulation along the blade varied elliptically. The lift and drag sectional data could then be modified for the effect of aspect ratio giving,
the three dimensional lift slope

$$\left(\frac{C_L}{\alpha}\right)_{3D} = \left(\frac{C_L}{\alpha}\right)_{2D}\left(\frac{\pi A}{1+\pi A}\right) \tag{33}$$

the three dimensional drag coefficient

$$(C_D)_{3D} = (C_D)_{2D} + \frac{(C_L)^2_{2D}}{\pi A} \tag{34}$$

where A was the aspect ratio of the blades.

Table 3 Estimated Sectional Data for a 3-D NACA 0012 Aerofoil (Elliptical loading)

Aspect Ratio=5

α	C_L	C_D
0	0.0	0.0180
1	0.094	0.0186
2	0.188	0.0200
3	0.291	0.0236
4	0.395	0.0287
5	0.489	0.0352
6	0.573	0.0430
7	0.658	0.0532
8	0.710	0.0648
9	0.743	0.0752
10	0.766	0.0978
12	0.810	0.1300

Aspect Ratio=10

α	C_L	C_D
0	0.0	0.0180
1	0.097	0.0183
2	0.194	0.0188
3	0.300	0.0206
4	0.407	0.0231
5	0.504	0.0266
6	0.591	0.0313
7	0.678	0.0376
8	0.732	0.0466
9	0.766	0.0554
10	0.790	0.0766
11	0.795	0.1114
12	0.810	0.1300

These effects were applied to the sectional data below stall. The modified sectional data is shown in Table 3 for aspect ratios of 5 and 10.

The results of the calculations using this data are shown in Figures 13a, b and c, for a propeller with the following particulars.

Radius	=0.1m
Maximum blade pitch angle	$=20^0$
No. of blades	=3
Free stream velocity	=2.0m/s
Root chord	=0.05m
Tip chord	=0.03m straight taper
Span	=0.1, 0.2, 100.0
Aspect Ratio	=5, 10, ∞ (including image effect)

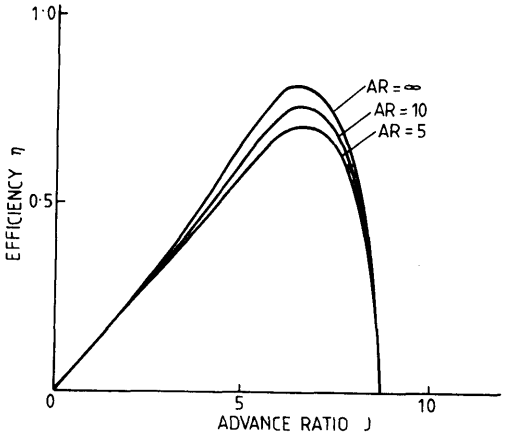

a. Efficiency η

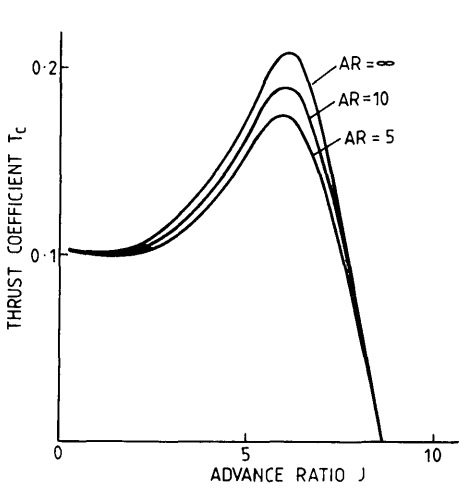

b. Thrust Coefficient Tc

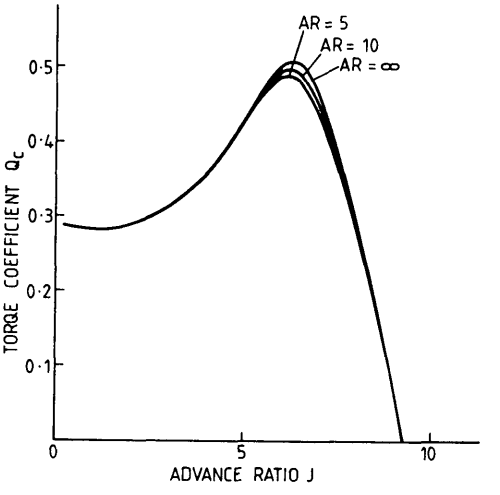

c. Torque Coefficient Qc

Fig. 13 Finite Span Rotary Foil Propeller-Comparison of Aspect Ratio

The curves for an infinite aspect ratio, and aspect ratios of 5 and 10 are plotted. The effect of aspect ratio is to reduce the maximum peak efficiency by approximately 7% for aspect ratio 10 and 14.5% for aspect ratio 5 from the two-dimensional result. The thrust coefficient was reduced by 9% for aspect ratio 10 and by 16% for aspect ratio 5.

6. Full Scale Propeller

Equation (25) for the thrust coefficient can be manipulated to give an expression for the required swept area of a propeller in terms of thrust, speed,

advance ratio and thrust coefficient.

$$Area=\frac{1}{\rho\pi^2}\left(\frac{T}{V_A{}^2}\right)\left(\frac{J^2}{T_c}\right) \tag{35}$$

where V_A the speed of advance replaces the free stream velocity for a propeller behind a ship. The first bracketed term is a function of a given ship, the second bracketed term describes the propeller characteristics.

For the finite span propeller of aspect ratio 5 described in the previous section, at J=6.0, T_c=0.175, Q_c=0.485 and η=0.69. Hence,

$$\frac{J^2}{T_c}=205.7$$

and $$\text{Area}=\frac{205.7}{\rho\pi^2}\left(\frac{T}{V_A{}^2}\right)=0.02\left(\frac{T}{V_A{}^2}\right)$$

where the density of seawater has been taken as 1025 kg/m³.

As an example consider a coaster LBP=66.0m, Beam 10.5m, Depth 5.2m, existing propeller diameter 2.65m, operating at 12 knots with an approximate thrust power of 470kW. Assuming w=0.15 and that w and t are the same for both propellers (w, t would actually be less for the rotary fiol propeller because it would operate in more open water due to its larger size).

$$\text{The required swept area}=\frac{0.02\times470\times10^3}{5.24^3}=65\text{m}^2$$

If the diameter of the new propeller is also 2.65m, the span required is 24.5m which is over twice the beam of the ship and clearly impracticable. This situation could be improved by increasing both the propeller solidity and the maximum blade pitching angle. If for example J^2/T_c is doubled, all other factors remaining constant, the span drops to 12.3m.

7. Conclusion

A multiple stream tube theory was developed for a rotary foil propeller. The theory was used for a series of parametric studies on two dimensional propellers. A three dimensional correction was added into the theory by assuming an elliptical variation of lift with blade span. The main findings were :

1) Higher efficiency was obtained with a trochoidal blade angle variation than with a sinusoidal blade angle variation. This higher efficiency was maintained over a large range of maximum blade oscillation angle.
2) With the foil section data used (NACA 0012 at $R_n=8\times10^4$) the maximum propeller efficiency attained was 0.82 at a propeller solidity of 0.9. This occurred at a maximum blade oscillation angle of 20 degrees and an advance ratio of 6.5.
3) Variation of propeller solidity had only a small effect on maximum efficiency. Thrust and torque coefficients were found to vary more or less

linearly with solidity.

4) Blade normal forces were found to vary approximately sinusoidally with propeller rotation angle. Blade tangential or in-line forces varied approximately as $sin\left(\frac{3\theta}{2}\right)$ with propeller rotation angle (θ).

5) Power, thrust and vertical force were found to have an oscillatory component during the cycle of rotation of the propeller. In general, the amplitude of this oscillation decreased as the number of blades increased.

6) Mean vertical force was found to have a small upwards value for a trochoidally varying blade oscillation.

7) Finite span was found to reduce efficiency, thrust coefficient and to a lesser extent torque coefficient. A drop of approximately 7% in efficiency and 9% in thrust was estimated for a propeller with blades of aspect ratio 10 ; 14.5% in efficiency and 16% in thrust respectively for a propeller with blades of aspect ratio 5.

8) Although high efficiencies are obtained with these propellers, they occur at high values of advance ratio and low thrust coefficient. Very large propeller swept areas are required for useful levels of thrust to be generated.

9) The effects of unsteady flow acting around the propeller blades have been neglected in this study. The results can be considered to be a 'first shot' approach to the calculation of the performance of a rotary foil propeller.

This report summarises the research work carried out by Neil Bose at the Ship Research Institute during the period October 12th 1986 to December 20th 1986. The work was carried out with the support of a Japanese Government Research Award for Foreign Specialists from the Science and Technology Agency.

Acknowledgements

The author would like to thank all the many people who made his stay in Japan a memorable one and in particular Dr. K. Sugai, Dr. H. Tanaka, Dr. Y. Ukon and Mr. T. Kudo of the Ship Research Institute, Mitaka, Tokyo, without whom this period of research would not have been possible.

The author would also like to thank the Science and Technology Agency of the Government of Japan for providing the majority of the funding under which this research was carried out, the University of Glasgow for approving this period of study leave and Professor D. Faulkner for his support to the plans.

References

1) Strickland, J.M. : "A Performance Prediction Method for the Darrieus Wind Turbine", Proceedings of the International Symposium on Wind Energy Systems, Cambridge, U.K., 1976.

2) Shankar, P.N. : "On the Aerodynamic Performance of a Class of Vertical Shaft Windmills", Proceedings of the Royal Society, London, A349 pp35-51, 1976.
3) Read, S. and Sharpe, D.J. : "An Extended Multiple Streamtube Theory for Vertical Axis Wind Turbines", Proceedings of the 2nd British Wind Energy Association Wind Energy Workshop, Cranfield, U.K., April 1980.
4) Sharpe, D.J. : "Refinements and Developments of the Multiple Streamtube Theory for the Aerodynamic Performance of Vertical Axis Wind Turbines", Proceedings of the 6th British Wind Energy Association Conference, Reading, 1984.
5) Sharpe, D.J. : "An Aerodynamic Performance theory for the Darrieus Wind Turbine", International Symposium on Wind Energy Systems, September 1976, Cambridge.
6) Critzos, C.C., Heyson, H.H. and Boswinkle, R.W. : "Aerodynamic Characteristics of NACA 0012 Airfoil Section at Angles of Attack from 0^0 to 180^0, NACA Tech Note 3361, 1955.
7) Jacobs, E.N. and Sherman, A. : "Airfoil Characteristics as Affected by Variations of the Reynolds Number", NACA Rep. No. 586.
8) Abbott, I.H. and Von Doenhoff, A.E. : "Theory of Wing Sections", Dover, 1959.